

CHAPTER 5

Longshore Current Forcing at a Barred Beach

D.J. Whitford¹ and E.B. Thornton², Member ASCE

1. Introduction

A local alongshore momentum balance was measured at various locations across a barred surf zone during the SUPERDUCK experiment held at the U.S. Army Corps of Engineers, CERC Field Research Facility (FRF), DUCK, N.C., U.S.A. on October 16, 1986. A mobile sled was instrumented to measure the various terms in the alongshore momentum equation. Numerically orienting the instrumentation perpendicular to the local bottom contours, the alongshore momentum balance simplifies to:

$$\frac{\partial M_y}{\partial t} + \frac{\partial S_{yx}^T}{\partial x} = \tau_y^n - \tau_y^b \quad (1)$$

where the terms represent (left to right) the temporal change of the time-averaged, depth-integrated mean momentum per unit area in the alongshore direction (M_y) due to both steady (\bar{M}_y) and unsteady (M_y') flow, the cross-shore gradient of the total alongshore momentum flux, surface wind stress, and bottom shear stress.

Three vertically and horizontally separated Marsh-McBirney bi-directional electromagnetic current meters, a Paroscientific digiquartz pressure sensor, and a single-point R.M. Young wind monitor, all mounted on a moveable sled, were used to measure current, wave and wind conditions in the surf zone. Spatially-dependent bed shear stress coefficients were determined as residuals from the alongshore momentum balance.

2. Experimental Site

The FRF site is located along a 100-km unbroken stretch of barrier island formation known as North Carolina's "Outer Banks." There are no littoral barriers to perturbate incoming wave trains along the entire reach of shoreline. The site has a tidal range of 0.5 to 2.0 m and regular offshore bathymetry. On October 16, the beach had a mean foreshore slope of 0.06, a single alongshore linear bar system, and a mean slope of 0.02 offshore of the

¹Fleet Numerical Oceanography Center, Monterey, CA, 93943 U.S.A.; formerly of Naval Postgraduate School, Monterey, CA, 93943, U.S.A.
²Naval Postgraduate School, Monterey, CA, 93943 U.S.A.

bar.

Sled instrumentation and deployment were described in Martens and Thornton (1987). Current meters were mounted at approximately 0.5 m, 1.0 m, and 1.5 m above the sled bottom. A Paroscientific digiquartz pressure sensor was used to infer surface elevation and mean water depth.

Daily bathymetric profiles of the experiment site were accurately measured with a Zeiss Elta-2 laser surveying system which sighted on the FRF Coastal Research Amphibious Buggy (CRAB) as it methodically traversed the experiment area. Precise orientation of the sled was achieved to within 0.5° using the laser surveying system to triangulate on two reflective prisms mounted approximately 2 m apart on a mast spreader above the sled.

Sled sensor measurements were acquired during 9 transects of the surf zone over a 7-day period. This paper discusses only a single transect accomplished on 16 October, as the additional transects are currently undergoing analysis. Wind speeds measured at 10 m elevation ranged from 10 to 12 ms⁻¹ and offshore H_{mo} ranged from 1.4 to 1.6 m. The transect consisted of 5 positions across the surf zone - outside the surf zone, at the point of maximum wave breaking, immediately before the bar, on top the bar, and in the bar-trough. Data were acquired at each position for approximately 35 minutes.

3. Momentum Balance Term Formulation

a. Temporal variability of mean longshore currents - Mean alongshore momentum is formulated from:

$$M_y = \overline{M_y} + M_y' = \rho V D + \int_{-h}^{\eta} \rho v' dz \quad (2)$$

where ρ is water density, V and v' are the mean and fluctuating components of the longshore current, D is the mean water depth, η is sea surface elevation and the over-bar denotes time averaging. Finite differencing in time was examined by varying the time step from 1-22 minutes, with and without a running mean.

b. Cross-shore gradient of alongshore momentum flux - Alongshore momentum flux (or radiation stress) is calculated using a linear wave theory transfer function:

$$S_{yx}(f) = |H(f)|^2 C_{uv}(f) \quad (3)$$

$$|H(f)|^2 = \frac{\rho[\sinh(2kh) + 2kh]}{4k[\cosh^2 k(h + z_m)]}$$

where C_{uv} is the co-spectrum of the current velocity components (u, v), f is frequency, k is wavenumber, h is mean water depth, and z_m is the measurement depth. Finite differencing in space is taken over the horizontal

distance between sled run positions, varying between 13-51 m. S_{yx}^T is the summation of $S_{yx}(f)$ over the sea-swell frequency band (0.06-0.44 Hz).

c. Surface wind stress -The alongshore component of surface wind stress (τ_y^N), hereafter referred to as simply 'surface wind stress', is calculated using the drag coefficient method (also called the bulk coefficient method):

$$\tau_y^N = \rho_a C_{d10} |U_{10}| U_{10y} \quad (4)$$

where ρ_a is air density, C_{d10} is a stability-dependent atmospheric drag coefficient for an elevation of 10 m, and U_{10} and U_{10y} are the total and alongshore components of wind speed measured by the sled anemometer, with atmospheric stability conversion to $z = 10$ m. During the SUPERDUCK experiment, Sethu Raman et al. (1987) calculated wind stress (τ^N) by the eddy correlation method using a three-component Gill anemometer. The wind speed measurements were acquired for $z_m = 18.7$ m at the seaward end of the FRF pier. This location was outside the surf zone and approximately 400 m from the sled transect area. Relative humidity, air, and sea surface temperature were also measured at the seaward end of the FRF pier. Atmospheric friction velocity (u_*) and the Monin-Obukhov length (L) were assumed spatially constant over both the surf zone and the end of the FRF pier. Onshore winds and unstable atmospheric conditions were predominant during the sled transect. A stability-dependent drag coefficient for the end of the FRF pier at a height of 10 m was calculated using:

$$u_* = (\tau^N / \rho_a)^{1/2} \quad (5)$$

$$U_{10} = U_{zm} - \frac{u_*}{\kappa} \left[\ln \frac{z_m}{10} + \psi_m \left(\frac{10}{L} \right) - \psi_m \left(\frac{z_m}{L} \right) \right] \quad (6)$$

$$C_{d10} = \tau^N / [\rho_a (U_{10} - U_0)^2] \quad (7)$$

where $\kappa = 0.4$ is von Karman's constant, ψ_m is an integral diabatic term for momentum, U_0 is the mean current (assumed negligible at the end of the FRF pier), and L is determined from the Businger et al. (1971) iterative approach. The increased surface roughness of a surf zone may be conservatively likened to the chaotic seas observed in advance of a cold front. Swell generated behind the cold front can travel through the front and interact with waves generated ahead of the front and propagating parallel to the front. This interaction results in a chaotic sea of larger, steeper waves and enhanced wave breaking. From a composite of wind stress measurements taken from multiple chaotic sea cases found in advance of storm fronts, the atmospheric drag coefficient was found to be increased by approximately 33% over that expected for non-chaotic seas of equal windspeed (Davidson et al., 1988a, 1988b). Atmospheric drag coefficients for the surf zone are therefore increased by

33% over that determined for the end of the FRF pier. Surf zone surface wind stress is then calculated from eqn. (4) and (6), where the C_{d10} and U_{10} are for the sled location. The substitution of $U_{10}-U_0$ for U_{10} in eqn. (4) for the surf zone surface wind stress made negligible difference.

d. Bottom shear stress - Bottom (or bed) shear stress is determined as the residual in eqn. (1). A bed shear stress coefficient (C_f) is then determined from:

$$C_f = \frac{\tau_b}{[\rho(u^2 + v^2)^{1/2}v]} \quad (8)$$

4. Sled Operation

The sled was deployed in an area of straight-and-parallel isobaths. The sled was towed offshore by the FRF's CRAB and dragged onshore with a tethered chain by a heavy-duty forklift. The sled's position and orientation were determined from laser surveys acquired at the beginning and end of each data run, with additional positioning surveys acquired during the run itself. Prior to sled deployment, a portable Zeiss laser ranging system was used to precisely determine the sled instruments' three-dimensional coordinates with respect to the sled prisms' three-dimensional coordinates. Laser surveys of the sled mast prisms during sled deployment provided precise location, sled pitch angle, and sled yaw angle to correct the sensor data with respect to the local horizontal and vertical. A mean bathymetric isobath orientation is determined by applying a least-squares regression fit to the bathymetric data. The sensors are then oriented with respect to this mean bathymetric isobath to determine cross-shore and longshore currents. Breaking waves were visually identified and electronically marked on the data tapes. The analog data were PCM encoded at the sled, telemetered ashore, decoded, and recorded on 9-track magnetic tape. The data were digitized at 8 Hz, demeaned and spectrally analyzed using Fast Fourier Transforms and ensemble averaging.

5. Data Analysis

Since S_{yx} is conserved outside the surf zone, any $S_{yx}(f)$ difference between the current meters measured outside the surf zone is assumed to be attributable to incorrect current meter alignment with respect to each other and the sled. Therefore, the rear current meter was numerically rotated until its $S_{yx}(f)$ coincided with the front current meter $S_{yx}(f)$. This 2.86° rotation was assumed to account for the alignment error and was fixed for the remaining data runs inside the surf zone.

Current meter calibration was conducted in flow tanks by different laboratories before and after the experiment. Current meter gain agreed within $\pm 3\%$ and current meter offset differed by only 0.01 - 0.04 ms^{-1} .

Homogeneity of surf zone currents is investigated by

overlying the bathymetry contours on both the mean current vectors determined at each sled run position and the mean current vectors determined from the fixed-bed current meters of an alongshore array (Figure 1). All current vectors have the same general direction and magnitude relative to their cross-shore position. No evidence of rip currents were seen visually during the sled transect nor are rip currents detected in Figure 1. Homogeneity of the surf zone current regime is therefore assumed for 16 October.

Stationarity is investigated by examination of S_{yx}^T calculated from measurements outside the surf zone acquired from a fixed-bed pressure and velocity sensor designated 'south tripod.' Sequential 34.1-minute spectra are calculated and resultant S_{yx}^T versus time are compared to the sled run transect times (Figure 2). In shallow water, $S_{xy} = \rho h \text{cov}_{uv}$. Ninety-five percent confidence limits for S_{yx}^T in Figure 2 are based on the Fisher-Z transformation (Miller and Freund, 1985):

$$Z = \frac{1}{2} \ln \left[\frac{1+r}{1-r} \right] \quad (9)$$

where the correlation coefficient (r) is

$$r = \frac{\text{cov}_{uv}}{\sigma_u \sigma_v} \quad (10)$$

and σ_u , σ_v are the standard deviations of u and v , and the covariance is calculated by integrating the co-spectrum of u , v . The Fisher-Z statistic is a value of a random variable having approximately a normal distribution. Unfortunately the 'south tripod' gage was not recording for the entire time of the transect. Therefore, stationarity is confirmed only for the first two runs of the transect and is assumed for the last three runs.

Relative contributions of wave forcing ($\partial S_{yx}^T / \partial x$), wind forcing (τ_y^n), and temporal variability of mean momentum ($\partial M_y / \partial t$) to the total momentum balance are determined by first defining their total contribution (TOT) as the cumulative sum of their absolute values:

$$\text{TOT} = \left| \frac{\partial S_{yx}^T}{\partial x} \right| + \left| \tau_y^n \right| + \left| \frac{\partial M_y}{\partial t} \right| \quad (11)$$

Their individual relative contributions (rc) are then determined by dividing by the total contribution:

$$\text{wave}_{rc} = \frac{\left| \frac{\partial S_{yx}^T}{\partial x} \right|}{\text{TOT}} \quad (12)$$

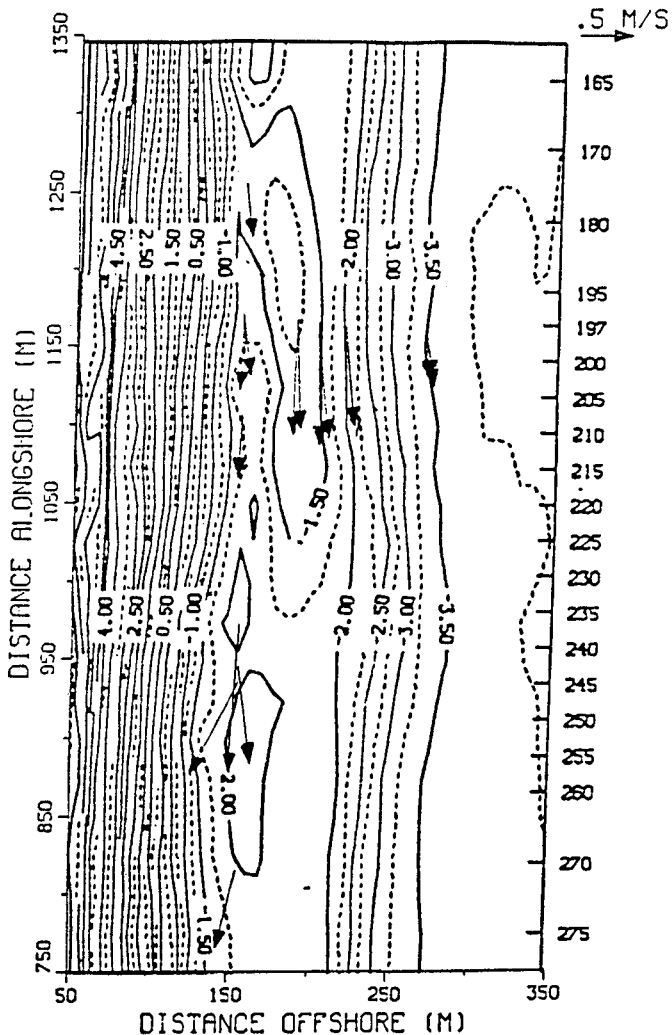


Figure 1. Sled and alongshore array mean current vectors for 16 October 1986 overlaid on bathymetry. Velocity scale is at upper right.

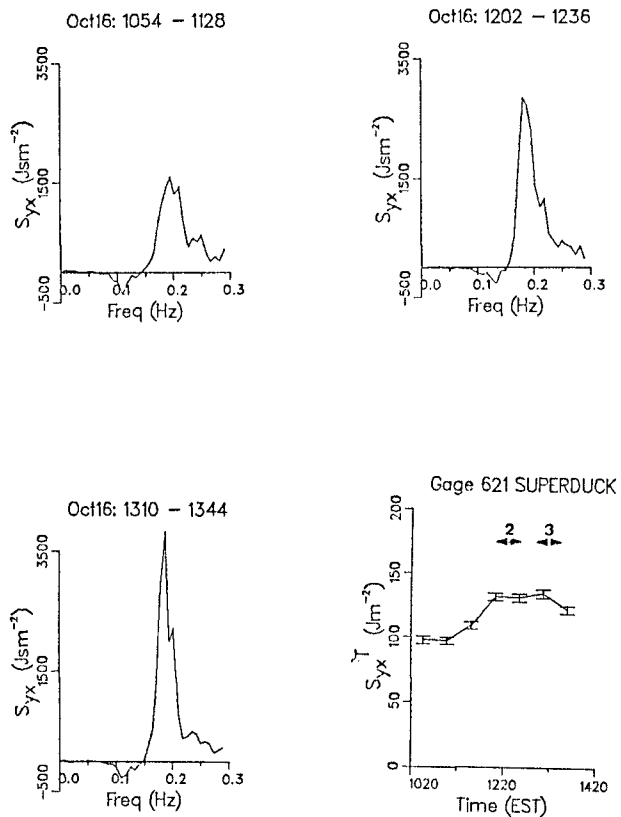


Figure 2. Offshore S_{yx} spectra and S_{yx}^T from 'puv' gage 621 for October 1986. Three representative S_{yx} spectra are shown. Numbers on S_{yx}^T figure indicate data runs. Intervals are 95% Fisher-Z confidence.

$$\text{wind}_{rc} = \frac{|\tau_y|}{TOT} \quad (13)$$

$$\frac{\partial M_y}{\partial t}_{rc} = \frac{\left| \frac{\partial M_y}{\partial t} \right|}{TOT} \quad (14)$$

An error analysis was conducted to place error bounds on the bed shear stress coefficients. Errors considered were beach angle orientation error, measurement error, finite differencing error, and an estimate of unquantified errors.

6. Results

Measured data and calculated results for all five data runs on 16 October are listed in Table 1. Three-dimensional portrayal of the mean current structure across the bar is illustrated in Figure 3. Current vectors represent 34.1-minute means and the numbers label data run locations. The short dotted lines above each run location indicate the mean water level (MWL) for each run and the long dashed line indicates mean sea level. The different arrowheads represent the three different current meter heights above the bed. Runs 16-4 and 16-5 had only two current meters totally submerged due to their shallow locations. The onset of breaking occurs between Runs 16-2 and 16-3.

Mean alongshore current [$0(1.0 \text{ ms}^{-1})$] dominates over the mean cross-shore current [$0(0.1 \text{ ms}^{-1})$]. Significant spatial variability is observed across the bar with strongest flow just before the bar and weakest flow in the trough and outside the breaker zone. The spatial distribution of the longshore current is of the same order as that found by Thornton and Guza (1986) for a planar beach, and thus the bar appears not to exert any major perturbation on the spatial variability of the flow from the trough to offshore. No measurements were taken inside the foreshore breakers where an additional peak (although of smaller magnitude) in mean longshore current would be expected. The substantial flow in the trough may be due to an along-shore pressure gradient (which was not measured) or turbulent mixing, since there was essentially no wave breaking occurring inside the trough between Runs 16-5 and 16-6. The current outside the breaker zone may be attributable to turbulent mixing. Offshore flow near the bed is noted for Runs 16-4 through 16-6. The vertical distribution of alongshore and cross-shore velocities is compared to normalized water depth (Figure 4). Current measurements for a single run are connected, with the numbers indicating the chronological run order (i.e., number 1 is run 16-2). Nearly depth-uniform flow is seen for the mean alongshore current, with a slight increase in velocity near the surface. A logarithmic velocity profile between current meter heights (0.5-1.5 m) was not found. However the data does not preclude a logarithmic profile over a different height

TABLE 1. Field experiment conditions on 16 October 1986

	Data Runs				
	16-2	16-3	16-4	16-5	16-6
1. Start time (E.S.T)	<u>1222</u>	<u>1318</u>	<u>1406</u>	<u>1449</u>	<u>1536</u>
2. h (m)	3.33	1.89	1.51	1.54	1.91
3. H_{rms} (m)	0.98	0.80	0.57	0.52	0.49
4. H_{m0} (m) from FRF gage 630	1.59	1.53	1.46	1.41	1.35
5. 1α	19°	15°	12°	19°	10°
6. $2Q(\%)$	0	12	5	3	1
7. S_{yx}^T (Jm^{-2})	250.5	151.0	57.2	48.0	25.9
8. U_{10} (ms^{-1})	12.3	11.4	10.9	10.2	10.0
9. 3θ	030°	027°	025°	026°	026°
10. $4C_f$	0.003 ± 0.0010	0.004 ± 0.0010	0.001 ± 0.0006	0.001 ± 0.0003	0.002 ± 0.0003
11. x-coord (m)	269.3	218.8	201.1	188.1	154.6
12. y-coord (m)	1157.4	1162.3	1165.2	1166.6	1170.4
13. cross-shore current (ms^{-1}):					
upper	0.09	0.12	-0.26	-0.25	-0.03
mid	0.04	0.10	0.03	-0.02	0.03
lower	0.08	0.09	0.12	0.05	0.08
14. longshore current (ms^{-1}):					
upper	-0.53	-1.09	-0.95	-0.91	-0.75
mid	-0.44	-0.98	-1.21	-1.13	-0.64
lower	-0.44	-0.99	-1.16	-1.07	-0.60
15. relative contributions (%) to momentum balance					
$\partial S_{yx}^T / \partial x$	87	95	77	70	81
$\frac{\eta}{\tau_y}$	8	3	19	18	2
$\partial M_y / \partial t$	4	2	3	12	17
16. $C_d(10^{-3})$	1.5	1.6	1.6	1.8	1.9

- Wave incident angle relative to beach normal
- Percent of waves which are breaking
- Wind direction relative to true north
- The C_f value noted is for the distance between the run indicated and the next run shoreward.
- Peak frequency in both the η and S_{yx} spectra for all runs was 0.19 Hz

SUPERDUCK
16 Oct 86
Profile 197

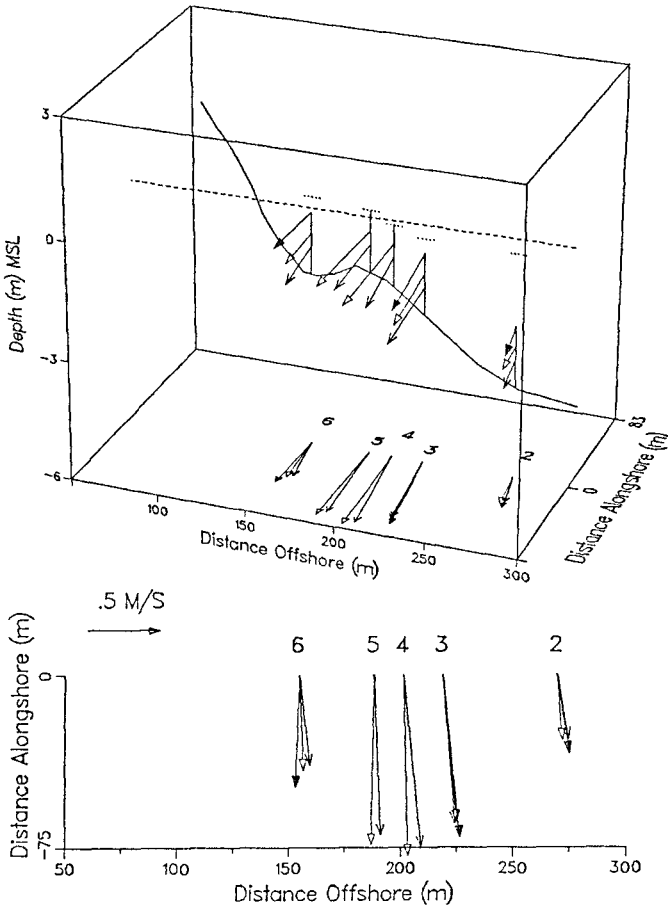


Figure 3. Mean current structure across the bar on 16 October 1986. Numbers represent data runs, short dotted lines are MWL's, and distance alongshore is arbitrary.

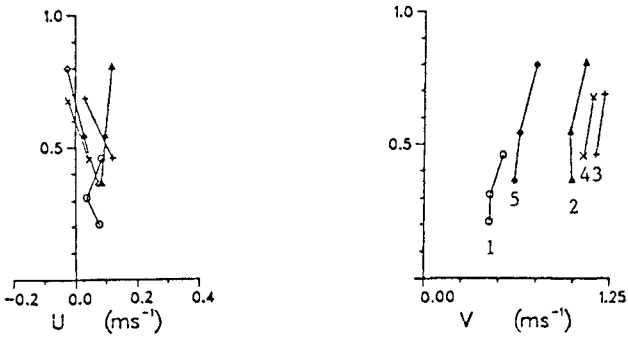


Figure 4. Mean cross-shore U and alongshore velocity V profiles versus normalized water depth for 16 October. Numbers on V profile indicate chronological sequence of data runs (e.g., 1 is Run 16-2).

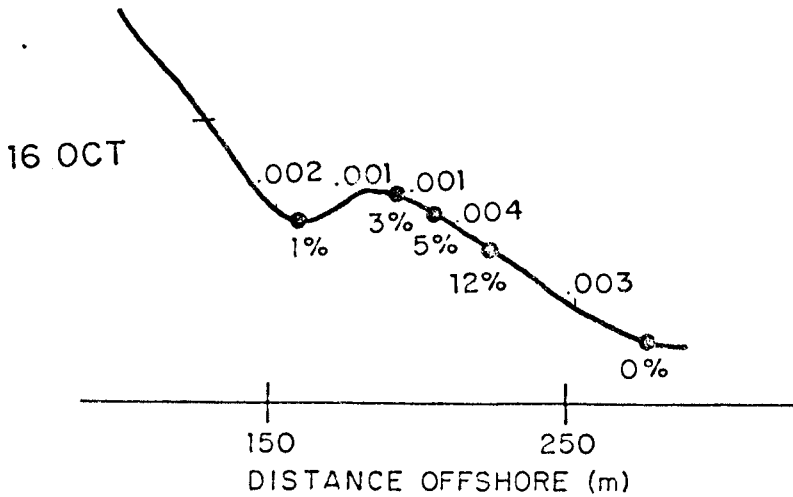


Figure 5. Bed shear stress coefficients (C_f) and percent breaking wave (Q) values as a function of offshore distance (C_f is above and Q is below the profile line).

interval (e.g., 0.0-1.0 m). The mean cross-shore flow exhibits a tendency for onshore flow in the upper third of the water column and offshore flow in the lower third of the water column.

The mean momentum due to the waves (M_y') was found to be less than an order of magnitude of the mean momentum due to the steady flow (M_y). Varying the time step for the temporal term (as discussed in paragraph 3a) made negligible difference, therefore Δt was arbitrarily assigned as 64 seconds.

Spatially-variable bed shear stress coefficients, calculated for the distance between run positions, and the percentage of waves which were breaking at each run position are indicated above and below the bathymetric profile in Figure 5. The bed shear stress coefficients are of $O(10^{-3})$ and are of the same order of magnitude as the model-fitted C_f values determined by Thornton and Guza (1986) using a non-linear formulation for bed shear stress. Spatial variability is indicated with higher C_f values offshore the bar and lower C_f values immediately before and on the bar. Grant et al. (1984) showed that C_f is increased by a factor of 2-3 due to the combined effect of waves and currents, therefore the shoreward decreasing C_f may be attributed to the shoreward decreasing surface wave action.

A surprising result was the low percentage of waves which were visually identified and marked as breaking waves. Visual identification of breaking was defined as when "white water" was observed passing the sled mast. For example, Run 16-3 was visually positioned in the surf zone at the point of maximum breaking (i.e., where the breaking wave heights were largest and therefore the maximum wave dissipation was occurring), yet only 12% of the waves were identified as breaking. Subsequent runs exhibited even less breaking wave occurrences.

The relative contribution of the radiation stress gradient to the momentum balance is observed to be highest at the two locations of maximum wave breaking - just before the bar (Run 16-3) and near the foreshore (Run 16-6). Surface wind stress' relative contribution doubles to nearly 20% in the trough, where wave breaking is reduced. The relative contribution of the temporal term increases shoreward from approximately 3% to a maximum of nearly 20% in the trough, perhaps due to the effect of infra-gravity waves and decreased wave breaking.

7. Summary

A local alongshore momentum balance is calculated from measurements of pressure, current, and wind acquired during a single transect of a barred beach during the SUPERDUCK experiment. Large incident wave angles (10° - 19°), combined with a highly accurate laser surveying system, signifi-

cantly reduced S_{yx} angular sensitivity which had plagued previous nearshore investigations and precluded accurate S_{yx} calculations. Surface wind stress is calculated using a stability-dependent atmospheric drag coefficient determined from wind stress measurements acquired during the field experiment. A three-dimensional depiction of surf zone currents indicates nearly depth-uniform mean alongshore flow with a slight increase in alongshore flow near the surface. Mean cross-shore flow indicates a tendency for onshore flow in the upper water column with offshore flow in the lower water column. Significant spatial variability of the alongshore flow is observed with maximum flow immediately offshore the bar. Spatial variability of the bed shear stress coefficient is observed with larger values offshore the bar (0.003-0.004) and lower values on the bar and in the trough (0.001). Relative contributions of wind forcing and the temporal term to the alongshore momentum balance are less than 10% offshore of the bar, where wave forcing was largest. However, relative contributions of wind forcing and the temporal term both approach 20% on the bar and in the trough. For this data set, wind forcing and the temporal term were not negligible terms in the momentum balance for locations on the bar and in the trough.

The information presented is the result of a single transect of the barred beach. A much more definitive conclusion should be reached after analysis of the remaining 8 transects of SUPERDUCK data.

8. Acknowledgments

Support for this field investigation and analysis was received from ONR under Contract NR 388-114. The staff of the U.S. Army Corps of Engineers, CERC Field Research Facility, Duck, N.C., assembled the sled and installed and maintained the offshore sensors and data acquisition system for the SUPERDUCK experiment.

9. References

- Businger, J. A., J. C. Wyngard, and Y. Izumi, 1971: Flux profile relationships in the atmospheric surface layer. J. Atmos. Sci., 28, 181-189.
- Davidson, K. L., P. J. Boyle, S. R. Fellbaum, and J. R. Mundy, 1988a: Atmospheric surface and mixed layer properties observed from ships in FASINEX. Proc. 7th A.M.S. Conf. on Air-Sea Interaction, 161-165.
- Davidson, K. L., W. J. Shaw, and W. G. Large, 1988b: Wind stress results from multi-platform and multi-sensor measurements in FASINEX. Proc. 7th AMS Conf. on Air-sea Interaction, Anaheim, CA, 132-136.
- Grant, W. D., A. J. Williams, III, and S. M. Glenn, 1984: Bottom stress estimates and their prediction on the northern California continental shelf during CODE-1: The

importance of wave current interaction. J. Phys. Oceanogr., 14, 506-507.

Martens, D. E. and E. B. Thornton, 1987: Nearshore zone monitoring system. Proc. Coastal Hydrodynamics Conf., ASCE, 579-588.

Miller, I. and J. E. Freund, 1985: Probability and Statistics for Engineers. 2nd ed., Prentice Hall, Inc., Englewood Cliffs, N.J., 530 pp.

Sethu Raman, S., M. J. Kang, C. E. Long, and J. M. Hubertz, 1987: SUPERDUCK Marine Meteorological Experiment, Data Summary Report, Vol. I (Mean Values) and Vol II, (Turbulence Parameters). U.S. Army Corps of Engineers, Coastal Engr. Rsch. Ctr., Waterways Experiment Station, Vicksburg, MS., (preliminary report, not yet published).

Thornton, E.B. and R.T. Guza, 1986: Surf zone longshore currents and random waves: field data and models. J. Phys. Oceanogr., 16(7), 1165-1178.